NOTES AND CORRESPONDENCE

On the Numerical Computation of Two-Dimensional Convective Flow

R. I. SYKES AND D. S. HENN

ARAP Division of CRT, Inc., Princeton, New Jersey

23 March 1987 and 11 June 1987

ABSTRACT

Numerical calculations of two-dimensional convection between flat plates at high Rayleigh numbers are presented. They do not show the large cell aspect ratios observed by Rothermel and Agee in their numerical calculations at high Rayleigh numbers. The present results appear to be insensitive to grid resolution, the conventional test of numerical accuracy, large amplitude random perturbations and the numerical representation of the diffusion term. We therefore suggest that the mechanism observed by Rothermel and Agee, which produces increasingly larger aspect ratio cells with increasing Rayleigh number, is strongly influenced by the numerical method used to solve the equations.

1. Introduction

In a recent paper, Rothermel and Agee (1986, referred to as RA hereafter) present results from a numerical study of the Benard–Rayleigh convection between parallel rigid walls and found an increased length scale for the convective motions at sufficiently large Rayleigh number. These results are of interest to meteorologists because they may suggest mechanisms for scale selection in atmospheric convection; the numerical model is two-dimensional and nonturbulent but contains some of the nonlinearity of the atmospheric case.

The purpose of this note is to present independent calculations of some of the flows reported by RA, using a different numerical model. Rothermel and Agee found that for Rayleigh numbers roughly from 10^4 to 10^5, the convective cells maintained a steady-state aspect ratio of approximately 3 (ratio of horizontal wavelength to vertical depth). At higher Rayleigh numbers of roughly 10^5 to 5×10^5, they obtained steady-state solutions with cell aspect ratios of approximately 10. We did not reproduce the large aspect ratio cells at the highest Rayleigh numbers and have been unable to resolve the discrepancy. We therefore present our results here, along with our supporting numerical evidence.

2. Numerical model

The equations of motion are the incompressible, Boussinesq form of the Navier-Stokes equations in two space dimensions as described in RA. The variables are nondimensionalized as in RA using the depth of the domain as a length scale and the diffusion timescale given by the domain depth squared divided by the diffusivity. Temperature is scaled by the temperature difference across the domain, which is held fixed. Since the Prandtl number is taken as unity, the only parameters in the problem are the Rayleigh number, R, and the length of the periodic domain in the horizontal. The boundary conditions on the fixed walls are free-slip.

We use a finite-difference discretization of the equations of motion, in contrast to the spectral representation of the horizontal structure employed in RA. The model is second-order accurate in space and time, employing leapfrog time differencing, the absolutely-conserving scheme of Piacsek and Williams (1970) for the nonlinear advection term and the Dufort-Frankel method for the diffusion term. One run, described in the next section, was made with a lagged explicit representation of the diffusion term as in RA. The weak nonlinear instability of the leapfrog scheme is suppressed by filtering the time-development slightly. A simple smoothing operator is used which combines each time-level with typically 2% of its neighbor. One of the runs (B2) in the next section was run with 1% smoothing to check sensitivity to this parameter. The elliptic equation for the pressure field is solved using an FFT to decompose the horizontal modes, and line inversion of the resulting tridiagonal matrix in the vertical.

The integrations were initialized with a small amplitude random perturbation to the linear temperature field, and the convective instability rapidly generates a finite amplitude field of motion.

Corresponding author address: Dr. R. Ian Sykes, A.R.A.P., 50 Washington Road, P.O. Box 2229, Princeton, NJ 08543-2229.

3. Results

We present our results for $R = 100R_c$, $400R_c$ and $800R_c$, where R_c is the critical Rayleigh number marking the onset of convective instability; $R_c \approx 657.5$ for the boundary conditions used here. While our $R = 100R_c$ run produces the same cell aspect ratio as RA, the higher Rayleigh number runs do not.

We have used the same domain as RA, i.e., a length of 28.28 units, which is chosen to accommodate 10 rolls at the onset of convective activity when $R = R_c$. For six out of the eight runs presented (A1–A3, B1–B3 in Table 1), the vertical grid is nonuniform, using 51 points to stretch smoothly from a spacing of 5×10^{-3} at the wall to 5×10^{-2} in the middle of the domain. The change in spacing from one point to the next is about 10% and the continuous grid variation preserves the second-order accuracy of the numerical scheme (Kalnay de Rivas 1972). The vertical grid for run B4 is also nonuniform, using 100 points to stretch from a spacing of 2.6×10^{-3} at the wall to 2.6×10^{-2} in the middle. Run B5 uses a uniform vertical grid spacing of 2×10^{-2}, similar to the finest grid of RA. The remaining numerical parameters are given in Table 1 for the various runs. The runs all reached a virtually steady state by the end of the integration period.

Figure 1 shows the time development of N, the number of cells in the computational domain for $R = 100R_c$ and $R = 800R_c$ (runs C1 and B2, respectively). The number of cells was determined by examining computer plots of the vertical velocity and temperature fields every 600 steps in the early stage of the run and every 6000 steps thereafter. The initial number of cells was obtained from the first set of plots where distinct cells could be distinguished. Since we have data only at the plotted times, we do not know the exact cell-merging process when N changed by more than one, e.g., a series of two-cell mergers or one multicell merger. It is seen that the early, rapid rate of cell merging agrees closely with that in RA's Fig. 1 for both values of R. While the final value of $N = 9$ agrees with RA for $R = 100R_c$, it does not for $R = 800R_c$, where RA obtained $N = 3$.

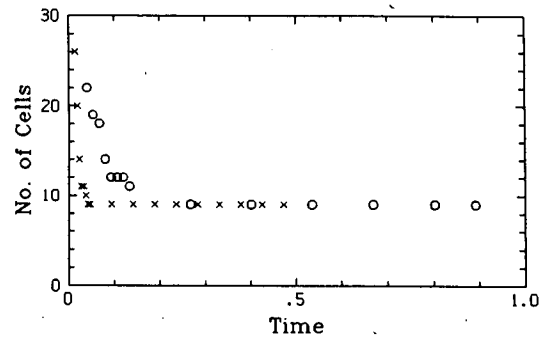

FIG. 1. Number of cells in computational domain as a function of time for $R = 100R_c$ (O) and $R = 800R_c$ (×).

Figure 2 shows the temperature fields from the two high horizontal resolution runs A3 and B3. The runs show 10 and 9 convection cells in the domain for $R = 400R_c$ and $R = 800R_c$ respectively, and both runs have actually maintained a constant number of cells since around $t = 0.05$. The rolls are not perfectly regular; there are spacing variations across the domain, and slight differences in detail between rolls. However, they do not appear to be subject to any instability, at least not on timescales on the order of the diffusion time or shorter. The lower resolution runs all show the same number of cells, but the details of the spacing vary slightly, presumably due to differences in the initial conditions.

The lower resolution runs are more than qualitatively similar, and Table 2 gives quantitative comparison between the runs. The best comparison is for the lower Rayleigh number, where three resolutions were tested, and it can be seen that doubling the number of grid nodes in the domain changes the Nusselt number and kinetic energy by about 1%. At the higher Rayleigh number, the differences are somewhat larger; there is a 2½% change in Nusselt number between B2 and B3. However, the differences are still small, and the three runs strongly suggest convergence of the numerical results with increasing resolution.

Further evidence for the convergence of the numerical solution is given in Fig. 3, which shows a horizontal section of the temperature structure in one downdraft

TABLE 1.

Run	$\frac{R}{R_c}$	Number of grid intervals in x	Number of grid intervals in Z	Timestep	Total time
A1	400	256	51	2.23×10^{-5}	0.535
A2	400	512	51	1.12×10^{-5}	0.859
A3	400	1024	51	1.12×10^{-5}	0.669
B1	800	256	51	7.89×10^{-6}	0.473
B2	800	512	51	7.89×10^{-6}	0.473
B3	800	1024	51	5.26×10^{-6}	0.615
B4	800	512	100	1.97×10^{-6}	0.315*
B5	800	512	52	7.89×10^{-6}	0.315*
C1	100	512	51	2.23×10^{-5}	0.669

* After initialization using B2 at time = .473.

TABLE 2.

Run	Nusselt number	Total kinetic energy KE	Max vertical velocity W_{max}
A1	17.0	3.05×10^6	710
A2	16.5	3.07×10^6	731
A3	16.3	3.04×10^6	733
B1	21.7	7.54×10^6	1129
B2	20.7	8.12×10^6	1166
B3	20.2	8.00×10^6	1175
B4	20.8	8.18×10^6	1167
B5	19.9	7.81×10^6	1142

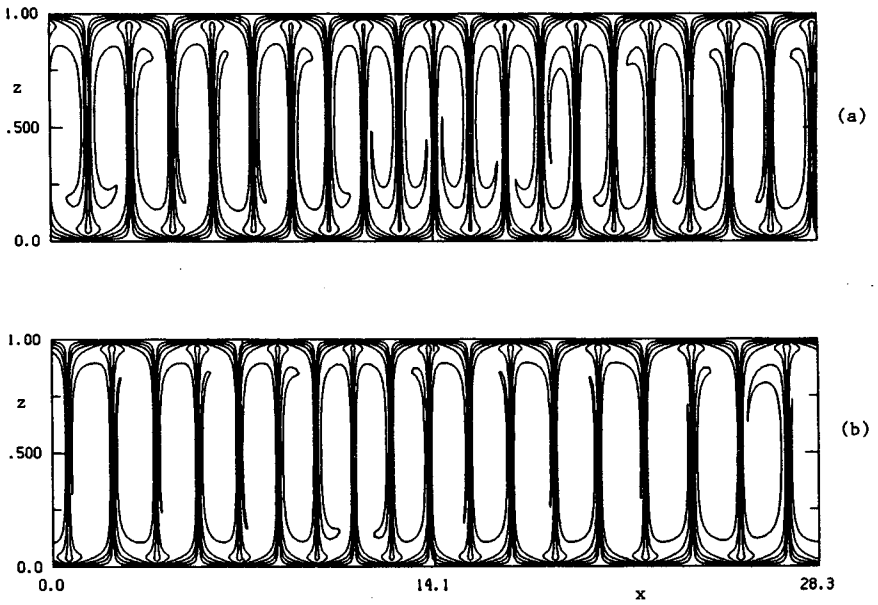

FIG. 2. Contours of the dimensionless temperature field at the end of the integration for the two high-resolution runs: (a) Run A3, $R = 400R_c$ and (b) Run B3, $R = 800R_c$. Contour interval is 0.125.

at $z = 0.5$ from the three runs with $R = 800R_c$. The temperature structure is the most difficult to resolve, so this example shows the worst aspect of the integration. The narrow plume of cold fluid is poorly resolved with 256 points, and produces significant grid-scale oscillations on both sides; it is perhaps surprising that run B1 produces heat transfer and kinetic energy levels so close to the higher resolution integrations and certainly suggests the need for a finer grid. The two higher resolution runs are much closer together, and the oscillation produced by the central differencing scheme has disappeared. The structure seems to be well resolved at the highest resolution, and it is interesting to note the small regions of warmer fluid flanking the cold downdraft. These can be seen in Fig. 2 also, and are caused by part of the adjacent warm updraft being entrained in the edges of the downdraft and being swept back down toward the lower boundary.

To test the stability of the solutions, among other things, we started runs B4 and B5 with initial fields

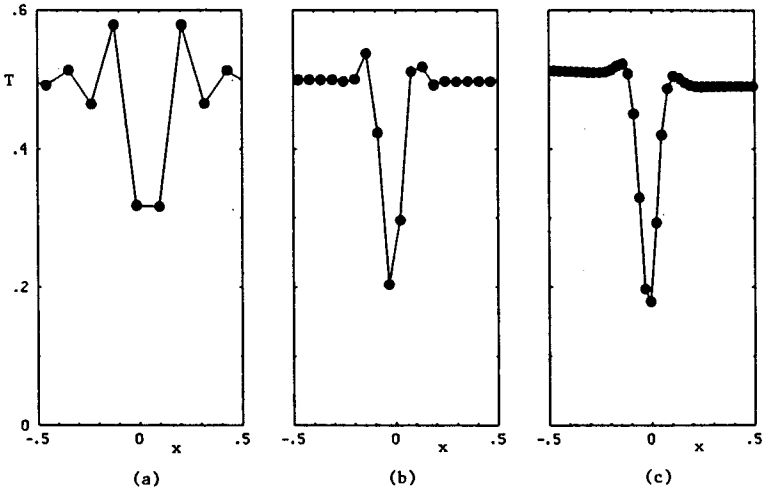

FIG. 3. Detailed cross section of the temperature structure in a single downdraft at $z = 0.5$ for $R = 800R_c$, showing the effect of increasing resolution: (a) Run B1, (b) B2, (c) B3. The horizontal coordinate is specified relative to the downdraft itself.

generated by interpolating the steady-state solution for the medium resolution $R = 800R_c$ run B2 on to the appropriate grids (which differ in the vertical) and adding a random disturbance of amplitude 0.25 to the temperature field. They were then run on to steady state. Run B4 was designed to test numerical convergence, especially with regard to the Dufort-Frankel scheme: the vertical spacing was halved while the time step was quartered compared to B2, as suggested by Richtmyer (1957). As mentioned previously, B5 has a uniform vertical grid and an explicit diffusion term representation and was designed to provide a numerical calculation as similar as possible to that of RA. In both cases, the number of cells remained the same as in B2. A quantitative comparison with B2 is given in Table 2. Run B4 strongly suggests numerical convergence with respect to vertical resolution and time step since the quantities in Table 2 all differ by less than 1% from B2. Considering the large change in vertical resolution near the wall, B5 indicates little sensitivity to the diffusion term representation; there is a 3.9% change in Nusselt number, a 3.8% change in kinetic energy and a 2.1% change in maximum vertical velocity.

4. Conclusions

We have presented numerical calculations of two-dimensional Benard–Rayleigh convection for the same external parameters as the calculations of Rothermel and Agee (1986), but have not obtained the same results. Our calculations do not show any significant increase in steady-state cell aspect ratio with increasing Rayleigh number up to $800R_c$. We have presented resolution tests to demonstrate reasonable convergence in our results, and we therefore believe that the different numerical representation is most likely responsible for the discrepancy. The fact that the large aspect ratios are only manifested at extremely high Rayleigh number, and even then on a relatively slow timescale indicates a very delicate mechanism; we suggest that further investigation is needed to resolve the effect of discretization schemes.

Acknowledgments. We would like to thank Drs. E. M. Agee and H. Segur for their help and encouragement in pursuing this study. This work was supported by the U.S. Office of Naval Research with R. F. Abbey as technical monitor.

REFERENCES

Kalnay de Rivas, E., 1972: On the use of non-uniform grids in finite difference equations. *J. Comput. Phys.*, **10,** 202.

Piacsek, S. A., and G. P. Williams, 1970: Conservation properties of convection difference schemes. *J. Comput. Phys.*, **6,** 392.

Richtmyer, R. D., 1957: Difference methods for initial-valve problems. Wiley-Interscience.

Rothermel, J., and E. M. Agee, 1986: A numerical study of atmospheric convective scaling. *J. Atmos. Sci.*, **43,** 1185.